

Structure of Chiral Phase Transitions at Finite Temperature in Abelian Gauge Theories

Kenji Fukazawa

Kure National College of Technology, Kure, Hiroshima 737- 8506, Japan

Tomohiro Inagaki

Information Processing Center, Hiroshima University, Higashi-Hiroshima,
Hiroshima 739-8526, Japan

Seiji Mukaigawa

Research Center for Nanodevices and Systems, Hiroshima University,
Higashi-Hiroshima, Hiroshima 739-8527, Japan

Taizo Muta

Department of Physics, Hiroshima University, Higashi-Hiroshima,
Hiroshima 739-8526, Japan

Abstract

The mechanism of the chiral symmetry breaking is investigated in the strong-coupling Abelian gauge theories at finite temperature. The Schwinger-Dyson equation in Landau gauge is employed in the real time formalism and is solved numerically within the framework of the instantaneous exchange approximation including the effect of the hard thermal loop for the photon propagator. It is found that the chiral symmetry is broken below the critical temperature T for sufficiently large coupling α . The chiral phase transition is found to be of the 2nd order and the phase diagram on the $T - \alpha$ plane is obtained. It is investigated how the structure of the chiral phase transition is affected by the hard thermal loops in the photon propagator.

1 Introduction

The chiral phase transition in gauge field theories at finite temperature is an interesting phenomenon in many respects. In particular it plays an important role when we deal with the early stage of the universe. It has been known for a long time that Abelian gauge theories at vanishing temperature subject to the chiral symmetry breaking in the strong coupling region and hence the massless fermions acquire a mass in a dynamical way [1, 2, 3, 4]. This phenomenon has been clarified mostly by using the Schwinger-Dyson equation [5].

It is quite natural from the point of view of the early universe to introduce the temperature effect in the analysis of the above phenomenon and see whether the broken chiral symmetry at vanishing temperature is restored at sufficiently high temperature and examine whether the phase transition is of the first order or second order. There have been several works dealing with this problem in quantum chromodynamics. There have, however, been not many works [6, 7, 8] which have studied this question by taking into account of the photon mass coming from the hard thermal loop. Thus we try to present the thorough analysis of the chiral phase transition in Abelian gauge theories at finite temperature with due consideration on the hard thermal loop by using the Schwinger-Dyson equation.

In our analysis we deal with the Schwinger-Dyson equation in the real time formalism to introduce the temperature [9, 10, 11, 12]. To solve the Schwinger-Dyson equation we confine ourselves to the instantaneous exchange approximation. The approximation is found to be valid in the high temperature region. In the case of the vanishing temperature the vacuum polarization effect is negligible. For high temperature the vacuum polarization becomes enhanced and so within our approximation we are forced to take into account of the vacuum polarization function in the photon propagator while dealing with the Schwinger-Dyson equation.

We make mostly numerical calculations in our analysis of the finite-temperature Schwinger-Dyson equation. We find that our numerical solutions are quite stable and the results are proven to be reliable. We find the clear signal of the second order chiral phase transition as temperature varies. We investigate the thermal photon mass effect in the chiral phase transition. We obtain critical curves on the $T - \alpha$ plane with T the temperature and α the fine structure constant.

2 Schwinger-Dyson equation at finite Temperature

Throughout the paper we work in Abelian gauge theories, in particular quantum electrodynamics, with massless fermions. The main purpose of our work is to see whether the broken chiral symmetry for large α at vanishing temperature is restored at high temperature and, if so, what is the nature of the chiral phase transition, i. e. whether the transition is of the 1st order or the 2nd order. Here α is the fine structure constant $\alpha = e^2/4\pi$ with e the electric charge of fermions. We rely on the Schwinger-Dyson equation in the real time formalism of the finite-temperature field theory. In the imaginary time approach the integral equation is cast into the infinite-component simultaneous equation and we do not prefer to cut off the summation in our calculation.

We start with the brief summary on the Schwinger-Dyson equation for vanishing temperature $T = 0$. The Schwinger-Dyson equation for the fermion self-energy part $\Sigma(p)$ reads within the ladder approximation in Landau gauge

$$\Sigma(p) = -ie^2 \int \frac{d^4q}{(2\pi)^4} \gamma^\mu iS(q) \gamma^\nu iD_{\mu\nu}^{tree}(p-q), \quad (1)$$

where $D_{\mu\nu}^{tree}(p-q)$ is the photon propagator at tree level and the self-energy part $\Sigma(p)$ is defined through

$$iS(p) = \frac{i}{\not{p} - \Sigma(p) + i\varepsilon} = \frac{i}{A(p^2)\not{p} - B(p^2) + i\varepsilon}, \quad (2)$$

with $S(p)$ the full propagator for massless fermions, and $A(p^2)$ and $B(p^2)$ the invariant functions of p^2 respectively. By the use of the invariant functions the self-energy part is represented such that $\Sigma(p) = (1 - A(p^2))\not{p} + B(p^2)$. It has been known for a long time [1, 2, 3] that Eq. (1) allows a non-vanishing

solution for $B(p^2)$ with $A(p^2) = 1$ if $\alpha > \alpha_c = \pi/3$. Thus the chiral symmetry is broken for the unusually large electromagnetic coupling and the massless fermion acquires the dynamical mass for $\alpha > \pi/3$.

At finite temperature in the real time formalism [9, 10, 11, 12] the full propagator for fermions may be written in the following form:

$$iS(p) = \frac{i}{\not{p}' - \Sigma(p) + i\varepsilon} = \frac{i}{A_0(p_0, |\vec{p}|)p_0\gamma^0 + A(p_0, |\vec{p}|)p_i\gamma^i - B(p_0, |\vec{p}|) + i\varepsilon}. \quad (3)$$

For simplicity we assume that

$$A_0(p_0, |\vec{p}|) = A(p_0, |\vec{p}|) = 1, \quad \text{Im}B(p_0, |\vec{p}|) = 0. \quad (4)$$

It will be seen that the above simplifying assumption does not lead to any inconsistencies. We then have

$$iS(p) = \frac{i}{\not{p}' - M(p_0, |\vec{p}|) + i\varepsilon}, \quad (5)$$

where the mass function $M(p_0, |\vec{p}|)$ is defined by

$$M(p_0, |\vec{p}|) = \frac{\text{trRe}\Sigma(p)}{\text{tr}1}. \quad (6)$$

In the closed time path method [12] the spinor self-energy part is given by the following matrix form:

$$i\Sigma^{ab}(p) = V^{-1}(\beta, p) \begin{pmatrix} i\Sigma(p) & 0 \\ 0 & -i\Sigma^*(p) \end{pmatrix} V^{-1}(\beta, p), \quad (7)$$

where $V(\beta, p)$ is the unitary matrix which connects the thermal vacuum to the zero-temperature vacuum and is given by

$$V(\beta, p) = \begin{pmatrix} \cos \varphi & -\epsilon(p_0) \sin \varphi \\ \epsilon(p_0) \sin \varphi & \cos \varphi \end{pmatrix}, \quad (8)$$

with

$$\cos \varphi = \frac{1}{\sqrt{1 + \exp(-\beta|p_0|)}}; \quad \sin \varphi = \frac{\exp(-\beta|p_0|/2)}{\sqrt{1 + \exp(-\beta|p_0|)}}. \quad (9)$$

Accordingly we find

$$\text{Re}\Sigma^{11}(p) = \text{Re}\Sigma(p), \quad (10)$$

and hence

$$M(p_0, |\vec{p}|) = \frac{\text{trRe}\Sigma^{11}(p)}{\text{tr}1}. \quad (11)$$

The Schwinger-Dyson equation in the real time formalism is written down in the matrix form within the framework of the closed time path method. If the vertex part is approximated by the tree form, the 1-1 matrix element of the equation is represented only by the 1-1 component of the fermion and photon propagator respectively and takes the following form,

$$\Sigma^{11}(p) = -ie^2 \int \frac{d^4q}{(2\pi)^4} \gamma^\mu iS^{11}(q) \gamma^\nu iD_{\mu\nu}^{11}(p-q). \quad (12)$$

Here the spinor two-point function $S^{11}(p)$ is given by evaluating the 1-1 matrix element of the expression [6, 7]

$$iS^{ab}(p) = V(\beta, p) \begin{pmatrix} S(p) & 0 \\ 0 & S^*(p) \end{pmatrix} V(\beta, p), \quad (13)$$

and reads

$$iS^{11}(p) = (y' + M(p_0, |\vec{p}|)) \left[\mathcal{P} \frac{i}{p^2 - M^2(p_0, |\vec{p}|)} + \pi \delta(p^2 - M^2(p_0, |\vec{p}|)) \tanh \frac{\beta |p_0|}{2} \right]. \quad (14)$$

The photon two-point function $D_{\mu\nu}^{11}(p)$ is also given by evaluating the 1-1 matrix element of the matrix

$$iD_{\beta}^{ab}(q) = U(\beta, q) \begin{pmatrix} D_{\mu\nu}(q) & 0 \\ 0 & D_{\mu\nu}^*(q) \end{pmatrix} U(\beta, q), \quad (15)$$

where

$$U(\beta, q) = \begin{pmatrix} \cosh \theta & \sinh \theta \\ \sinh \theta & \cosh \theta \end{pmatrix}, \quad (16)$$

$$\cosh \theta = \frac{1}{\sqrt{1 - \exp(-\beta |q_0|)}}; \quad \sinh \theta = \frac{\exp(-\beta |q_0|/2)}{\sqrt{1 - \exp(-\beta |q_0|)}}. \quad (17)$$

The general form of the photon propagator at finite temperature is well-known and is given by [11]

$$iD_{\mu\nu}(q) = \frac{i}{q^2 - \Pi^T(q) + i\varepsilon} P_{\mu\nu}^T + \frac{i}{q^2 - \Pi^L(q) + i\varepsilon} P_{\mu\nu}^L - i \frac{\alpha_{GF}}{q^2 + i\varepsilon} \frac{q_\mu q_\nu}{q^2}, \quad (18)$$

where $P_{\mu\nu}^T$ and $P_{\mu\nu}^L$ are the transverse and longitudinal projection operators respectively and α_{GF} is the gauge fixing parameter. Below we take the Landau gauge $\alpha_{GF} = 0$ which is consistent with the Ward-Takahashi identity within the ladder approximation at $T = 0$. We then find that

$$iD_{\mu\nu}^{11}(p) = \text{Re}D_{\mu\nu}(q) \coth \frac{\beta |q_0|}{2} + i \text{Im}D_{\mu\nu}(q), \quad (19)$$

where

$$\text{Re}D_{\mu\nu}(q) = \text{Re}D^T(q)P_{\mu\nu}^T + \text{Re}D^L(q)P_{\mu\nu}^L, \quad (20)$$

$$\text{Im}D_{\mu\nu}(q) = \text{Im}D^T(q)P_{\mu\nu}^T + \text{Im}D^L(q)P_{\mu\nu}^L. \quad (21)$$

with

$$\begin{aligned} \text{Re}D^T(q) &= \mathcal{P} \frac{-\text{Im}\Pi^T(q)}{(q^2 - \Pi^T(q))(q^2 - \Pi^{T*}(q))} \\ &+ \pi\varepsilon(q^2 - \text{Re}\Pi^T(q))(q^2 - \text{Re}\Pi^T(q))\delta((q^2 - \Pi^T(q))(q^2 - \Pi^{T*}(q))), \end{aligned} \quad (22)$$

$$\begin{aligned} \text{Re}D^L(q) &= \mathcal{P} \frac{-\text{Im}\Pi^L(q)}{(q^2 - \Pi^L(q))(q^2 - \Pi^{L*}(q))} \\ &+ \pi\varepsilon(q^2 - \text{Re}\Pi^L(q))(q^2 - \text{Re}\Pi^L(q))\delta((q^2 - \Pi^L(q))(q^2 - \Pi^{L*}(q))), \end{aligned} \quad (23)$$

$$\begin{aligned} \text{Im}D^T(q) &= \mathcal{P} \frac{q^2 - \text{Re}\Pi^T(q)}{(q^2 - \Pi^T(q))(q^2 - \Pi^{T*}(q))} \\ &+ \pi\varepsilon(q^2 - \text{Re}\Pi^T(q))\text{Im}\Pi^T(q)\delta((q^2 - \Pi^T(q))(q^2 - \Pi^{T*}(q))), \end{aligned} \quad (24)$$

$$\begin{aligned} \text{Im}D^L(q) &= \mathcal{P} \frac{q^2 - \text{Re}\Pi^L(q)}{(q^2 - \Pi^L(q))(q^2 - \Pi^{L*}(q))} \\ &+ \pi\varepsilon(q^2 - \text{Re}\Pi^L(q))\text{Im}\Pi^L(q)\delta((q^2 - \Pi^L(q))(q^2 - \Pi^{L*}(q))). \end{aligned} \quad (25)$$

Finally the Schwinger-Dyson equation at finite temperature in the real time formalism takes the following form

$$\begin{aligned}
M(p_0, |\vec{p}|) &= \frac{1}{\text{tr}1} \text{trRe} \left[-ie^2 \int \frac{d^4q}{(2\pi)^4} \gamma^\mu iS^{11}(q) \gamma^\nu iD_{\mu\nu}^{11}(p-q) \right] \\
&= -e^2 \int \frac{d^4q}{(2\pi)^4} M(q_0, |\vec{q}|) \\
&\quad \times \left[\mathcal{P} \frac{1}{q^2 - M^2(q_0, |\vec{q}|)} (2\text{Re}D^T(p-q) + \text{Re}D^L(p-q)) \coth \frac{\beta|p_0 - q_0|}{2} \right. \\
&\quad \left. + (2\text{Im}D^T(p-q) + \text{Im}D^L(p-q)) \delta(q^2 - M^2(q_0, |\vec{q}|)) \tanh \frac{\beta|q_0|}{2} \right], \tag{26}
\end{aligned}$$

where it should be noted that the following formulae have been employed,

$$\gamma^\mu \gamma^\nu P_{\mu\nu}^T = -2, \quad \gamma^\mu \gamma^\nu P_{\mu\nu}^L = -1. \tag{27}$$

3 Instantaneous exchange approximation

In order to derive informations on the phase structure of quantum electrodynamics at finite temperature as much as possible we try to solve the Schwinger-Dyson equation regarding it as an integral equation for the mass function $M(p_0, |\vec{p}|)$. To solve the equation it is inevitable to make some approximation which may not give any serious influence on the resulting physical predictions. Throughout the paper we apply the instantaneous exchange approximation in which the p_0 dependence of the relevant Green functions is assumed to be weak and is neglected. For photons the approximation implies that the vacuum polarization function is p_0 independent. As a functional form of the vacuum polarization function we adopt the one suggested by the hard thermal 1-loop calculation:

$$\Pi^T(q_0, q)|_{q_0 \rightarrow 0} \sim 0, \quad \Pi^L(q_0, q)|_{q_0 \rightarrow 0} \sim 2Nm_{ph}^2 \equiv \frac{N}{3}e^2T^2, \tag{28}$$

where N is the number of fermion flavors. With this approximation the Schwinger-Dyson equation is rewritten as

$$\begin{aligned}
M(p_0, |\vec{p}|) &= \pi e^2 \int \frac{d^4q}{(2\pi)^4} M(q_0, |\vec{q}|) \left(2\mathcal{P} \frac{1}{(\vec{p} - \vec{q})^2} + \mathcal{P} \frac{1}{(\vec{p} - \vec{q})^2 + 2Nm_{ph}^2} \right) \\
&\quad \times \delta(q^2 - M(q_0, |\vec{q}|)^2) \tanh \frac{\beta|q_0|}{2}. \tag{29}
\end{aligned}$$

Since the right-hand side of Eq.(29) has no p_0 dependence in this approximation, the mass function $M(p_0, |\vec{p}|)$ is independent of p_0 and so is written as $M(|\vec{p}|)$. Hence we obtain

$$\begin{aligned}
M(p) &= \frac{\alpha}{2\pi} \int q^2 dq \frac{M(q)}{\sqrt{q^2 + M(q)^2}} \\
&\quad \times \frac{1}{2pq} \left(2 \ln \frac{(p+q)^2}{(p-q)^2} + \ln \frac{(p+q)^2 + 2Nm_{ph}^2}{(p-q)^2 + 2Nm_{ph}^2} \right) \tanh \frac{\beta\sqrt{q^2 + M(q)^2}}{2}, \tag{30}
\end{aligned}$$

where we set $p = |\vec{p}|$ and $q = |\vec{q}|$. In the following sections we analyze Eq. (30) numerically by using computers and study the behavior of the mass functions to derive informations on the phase transitions.

4 Numerical solutions

We would like to solve Eq. (30) by the use of the numerical method. There are several different methods available for solving the integral equation (30) numerically. Among those methods there exist two standard

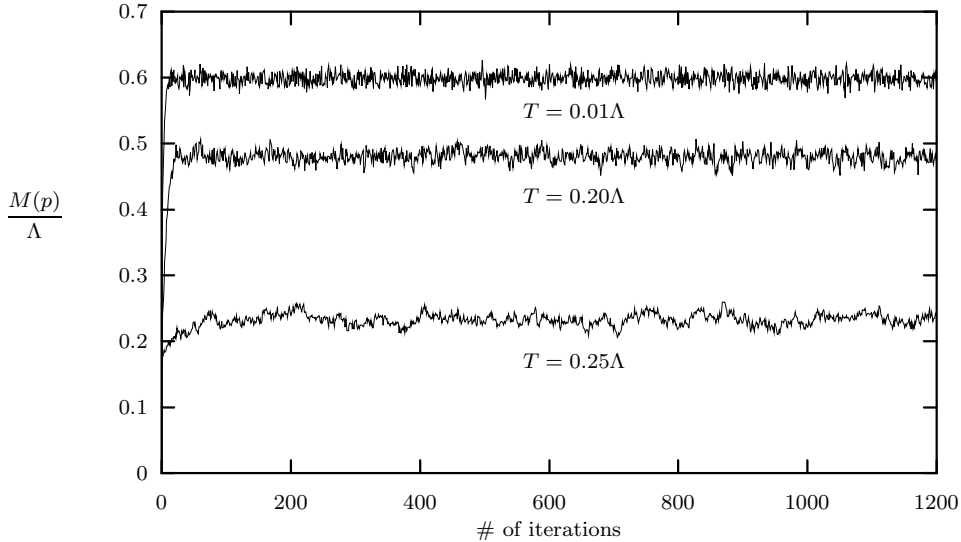


Figure 1: Typical behavior of the solution of Schwinger-Dyson equation (30) for $N = 0$, $\alpha = 1$, and $p = 0.1\Lambda$.

methods. The one is to discretize the integral in Eq. (30) and regard the resulting equation as simultaneous equations for the mass function. The other of the two is to start with the suitable trial function for the solution and to iterate it until we reach a stable solution. It seems that the latter method is much easier to handle and is useful as long as the convergence of the iteration is guaranteed. We would like to adopt this latter method in the following arguments.

We begin with the simplest possible choice for the trial mass function in the iteration. Thus the trial function is chosen to be a constant independent of p ,

$$M(p) = \text{constant}. \quad (31)$$

At each step of the iteration the integration is performed by the use of the Monte Carlo method and the integral is cut off at mass scale Λ . After the first iteration the resulting mass function acquires a p dependence and is substituted for the mass function in the integral on the right hand side of Eq. (30). Repeating this procedure we may have a possible stable result. Whether we have a stable result or not should be always checked after sufficiently many iterations. In each calculation in the following we confirm the stability of the solution, that is, we obtain the same result starting from the different trial functions.

We first consider the case without the thermal photon mass $N = 0$. Note here that parameter N plays a role of switching on ($N = 1$) and off ($N = 0$) the photon mass and also represents the number of fermion flavors. In Fig. 1 the mass function normalized by the cut-off Λ of the p integration is presented as a function of the number of the iterations for the case with $p = \Lambda/100$ and $T = 0.01\Lambda, 0.20\Lambda, 0.25\Lambda$. Here we adopt the unit system with $k = 1$ where k is the Boltzmann constant. The fluctuations observed in Fig. 1 are given rise to by the errors in the Monte Carlo integration.

As is seen in Fig. 1, the resulting mass function becomes stable after about 100 iterations. We then push forward our analysis by taking more points for the values of the momentum and obtain the momentum dependence of the solution for the mass function. In Fig. 2 the mass function normalized by the cut-off is presented as a function of the momentum p normalized by the cut-off. The mass functions were obtained after 1200 iterations. It should be noted here that the convergence of the iterations becomes slower if we sit near the critical value of the coupling constant α and temperature T . In this case we need more iterations to obtain a stable result for the mass function.

The case with the thermal photon mass $N = 1$ is studied essentially in the same way as above. We

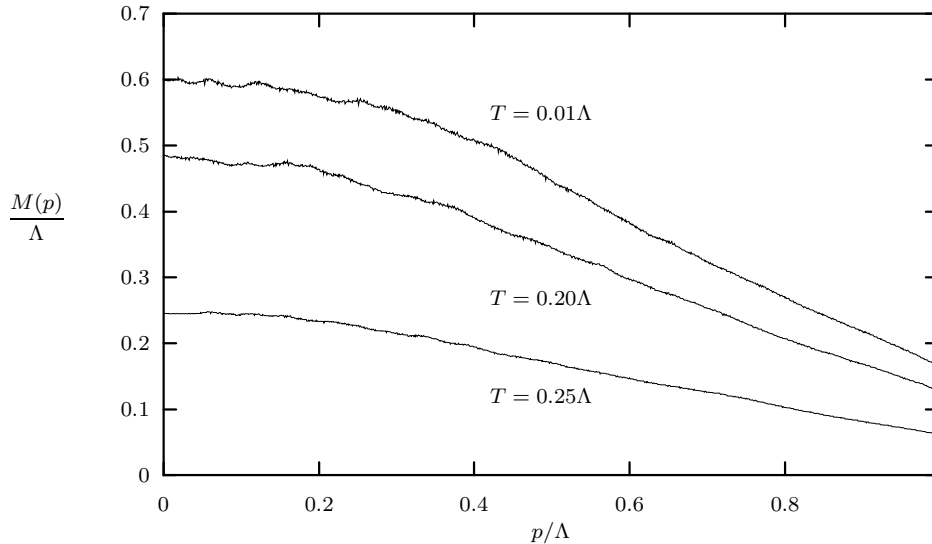


Figure 2: Typical shape of the mass function $M(p)$ for $N = 0$ and $\alpha = 1$.

may also study the case with three fermion flavors $N = 3$ essentially in the same manner. Here we skip to present the numerical results on the mass function.

5 Chiral phase transitions

We first wish to observe the behavior of the mass function at some fixed value of p as a function of parameters α and T . The α dependence of the mass function $M(p)$ with $p = 0.1\Lambda$ is shown in Fig. 3 for various fixed values of T . Note here that the errors coming from the fluctuations observed in Fig. 1 are smaller than the size of the mark shown for each sample point in Fig. 3.

As is clearly seen in Fig. 3, the chiral phase transition is of the second order since the fermion mass is generated at a critical value of the coupling constant α without any discontinuity. By picking up the critical value of α where the mass generation occurs one can obtain the critical parameters α_c and T_c respectively. If T_c is plotted versus α_c , we obtain the phase diagram. We shall come back to this subject later in Section 6. It should be noted here that the value of the critical coupling constant α_c for $T = 0$ is found to be 0.44477 ± 0.00053 (See Appendix A). This value differs from the well-known value $\pi/3$. The reason for this is simple, i. e., we applied the instantaneous exchange approximation in our approach which is not the good approximation in the low temperature region. Thus we have to be careful in applying our method and consider that our formulation is suitable rather in the high temperature region.

We can also observe the behavior of the mass function $M(p)$ at some fixed value of p as a function of temperature T . The T dependence of $M(p)$ with $p = 0.1\Lambda$ is given in Fig. 4 for fixed α . Here again we clearly observe the second order chiral phase transition in Fig. 4.

If the thermal photon mass is included ($N = 1$), the essential feature of the behavior of the mass function is more or less the same as in the case without the thermal photon mass. We present the α and T dependence of the mass function $M(p)$ are presented in Figs. 5 and 6.

We recognize that the behavior of the mass function in the low temperature region as seen in Figs. 4 and 6 is significantly different from the one in the case without the thermal photon mass. The similar behavior is observed in the case of $N = 3$ although the result is not shown in figures.

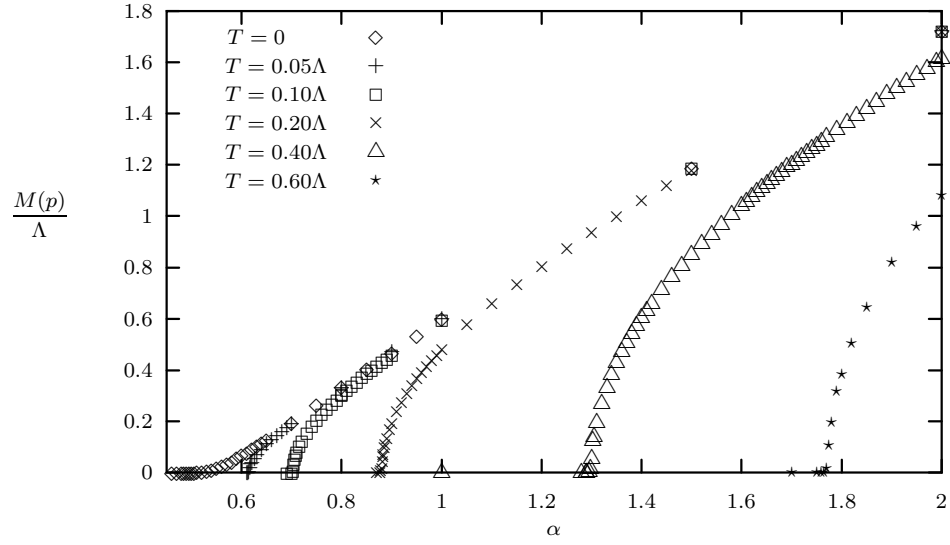


Figure 3: Dynamical fermion mass as a function of the coupling constant α for $N = 0$ at $p = 0.1\Lambda$

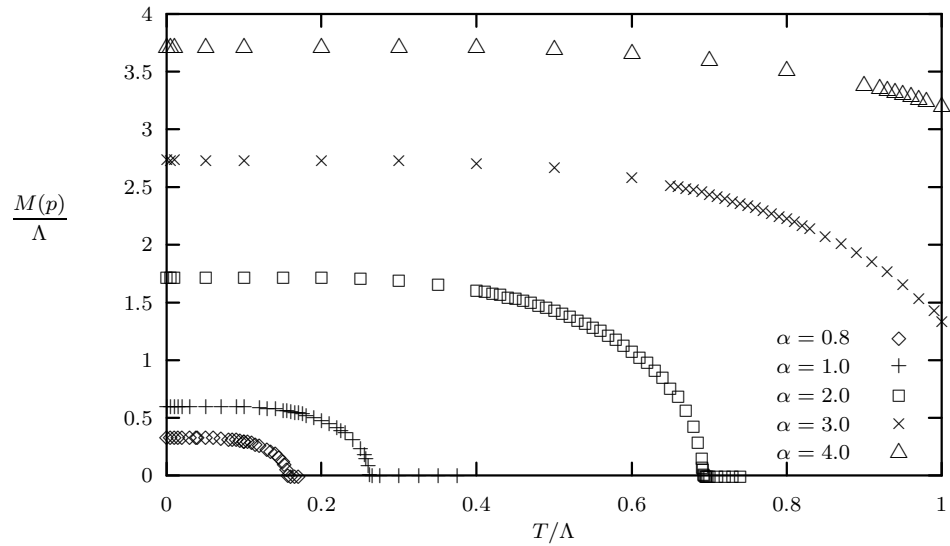


Figure 4: Dynamical fermion mass as a function of the temperature T for $N = 0$ at $p = 0.1\Lambda$

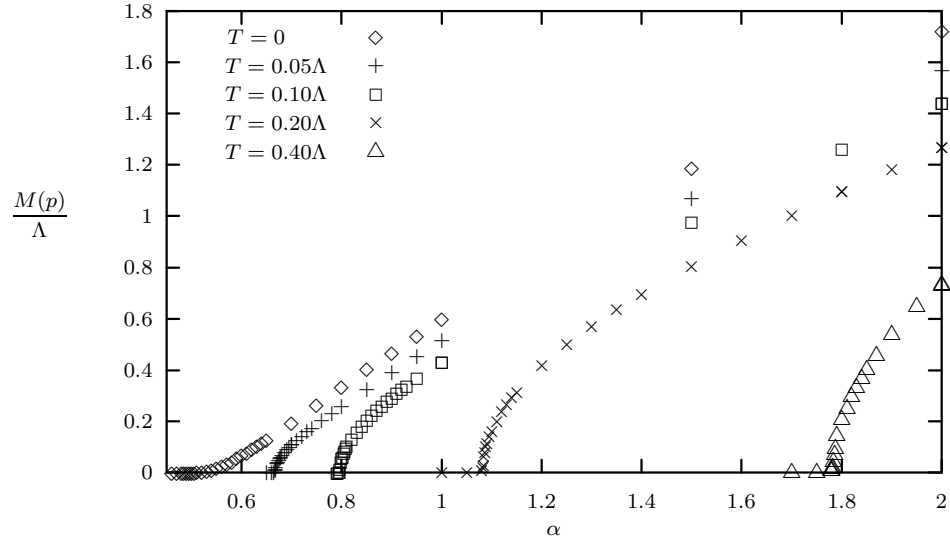


Figure 5: Dynamical fermion mass as a function of the coupling constant α for $N = 1$ at $p = 0.1\Lambda$

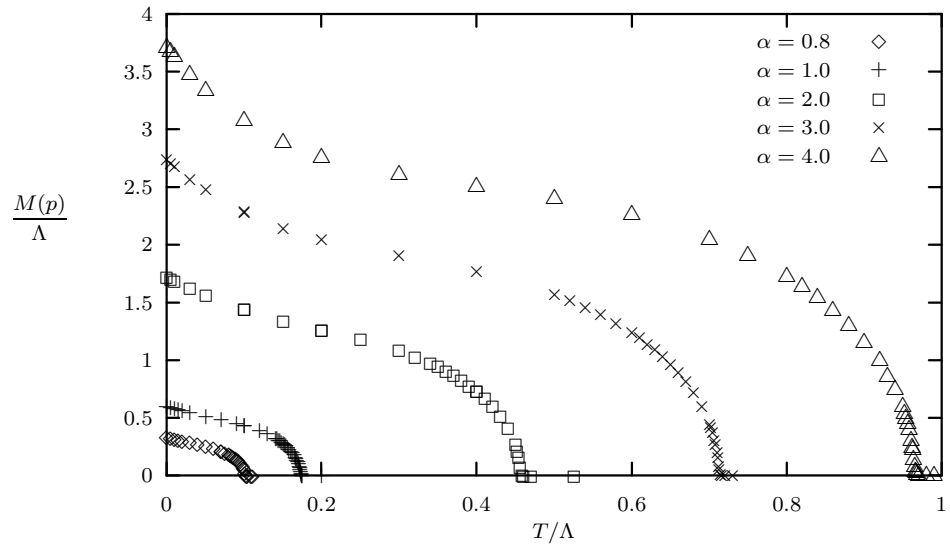


Figure 6: Dynamical fermion mass as a function of the temperature T for $N = 1$ at $p = 0.1\Lambda$

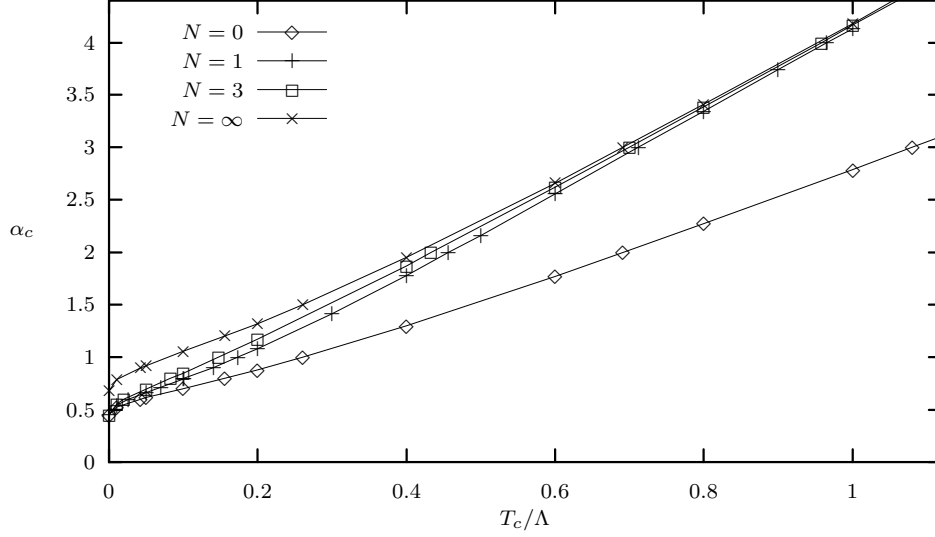


Figure 7: Critical curves for $N = 0, N = 1, N = 3$ and $N = \infty$ at $p = 0.1\Lambda$.

6 Critical curve and critical exponents

By observing the figures obtained in the last section we can directly draw the critical curve on the $T - \alpha$ plane. In fact, for the case with $N = 0$ we pick out the values of α where the mass function vanishes and plot those values as a function of temperature. The resulting curve is the critical curve for the case with $N = 0$. In order to perform this procedure in a more systematic way and to obtain critical exponents simultaneously we apply the following method.

We fit the function $M(p)$ with n data points M_i, α_i and T_i with $i = 1, \dots, n$ near the critical point by assuming the functional form of the function $M(p)$ such that

$$M(p) = e^{C_T}(\alpha - \alpha_c)^\nu, \quad (32)$$

for fixed temperature T and

$$M(p) = e^{C_\alpha}(T_c - T)^\eta, \quad (33)$$

for fixed coupling constant α respectively. Here $C_T, C_\alpha, \alpha_c, T_c, \nu$ and η are adjustable parameters with α_c and T_c corresponding to the critical coupling constant and critical temperature respectively and ν and η designate the critical exponent. To estimate the values of $C_T, C_\alpha, \alpha_c, T_c, \nu$ and η we adopt the familiar least-squares fit. We choose n data points near the critical point and minimize the quantities

$$\sum_{i=1}^n [\ln M_i - (\nu \ln(T_c - T_i) + C_T)]^2, \quad (34)$$

with temperature T fixed and

$$\sum_{i=1}^n [\ln M_i - (\eta \ln(\alpha_i - \alpha_c) + C_\alpha)]^2, \quad (35)$$

with coupling constant α fixed.

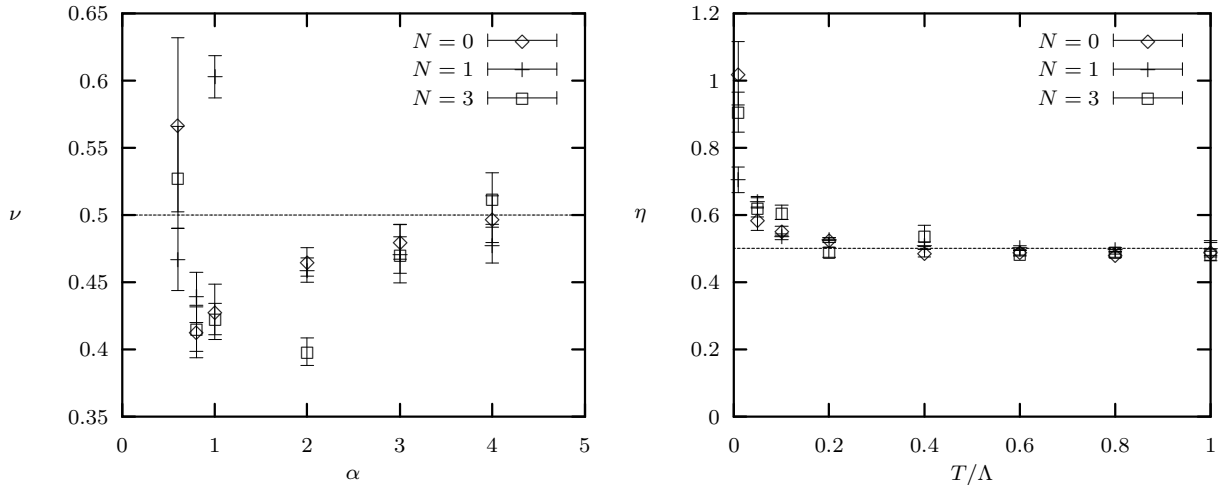


Figure 8: Critical exponents ν and η estimated at $p = 0.1\Lambda$.

The critical curves for $N = 0$, $N = 1$, $N = 3$ and $N = \infty$ are shown in Fig. 7. Taking the $N \rightarrow \infty$ limit in Eq. (30) we find that the dynamical fermion mass for $N = \infty$ is obtained by replacing α by $(2/3)\alpha$ in the case $N = 0$. Thus the critical coupling constant α_c for $N = \infty$ is given by α_c for $N = 0$ multiplied by $2/3$. The longitudinal mode of the photon propagator acquires the non-vanishing thermal mass for $N \neq 0$. Since the thermal photon mass m_{ph} tends to suppress the gauge interaction, it has an effect of protecting the chiral symmetry. As is seen in Fig. 7 the effect of the thermal photon mass enhances the critical coupling α_c and becomes stronger as T increases.

In Fig. 8 the critical exponents ν and η are shown as a function of the temperature and coupling constant respectively. As is seen in Fig. 8 the critical exponents do not depend on the number of fermion flavors N guaranteeing the accuracy of our numerical analysis. Taking the average of the critical exponents ν for $\alpha = 1, 2, 3, 4$ and η for $T/\Lambda = 0.2, 0.4, 0.6, 0.8, 1.0$ we obtain

$$\nu \sim \begin{cases} 0.46 & \text{for } N = 0, \\ 0.50 & \text{for } N = 1, \\ 0.45 & \text{for } N = 3, \end{cases} \quad (36)$$

and

$$\eta \sim \begin{cases} 0.49 & \text{for } N = 0, \\ 0.51 & \text{for } N = 1, \\ 0.49 & \text{for } N = 3, \end{cases} \quad (37)$$

respectively. Therefore our results are consistent with $\nu = 1/2$ and $\eta = 1/2$ which are in accord with the critical exponents in the four-fermion theory [18].

In Fig. 9 the N dependence of the mass function is presented. Since the longitudinal mode for photon propagator acquires the thermal mass for $N \neq 0$, the photon propagator has only one massless mode. On the other hand the photon propagator has three massless modes for $N = 0$. As is seen in Fig. 9 the dynamical fermion mass strongly depends on the number of massless modes in the photon propagator near the critical temperature where the instantaneous exchange approximation is valid.

Note that the behaviors of the critical curve and the dynamical fermion mass for finite N seem different from the results in Ref. [7]. In Ref. [7] the thermal photon mass is introduced both for the longitudinal and transversal mode. In this case there is no massless mode for the photon propagator.

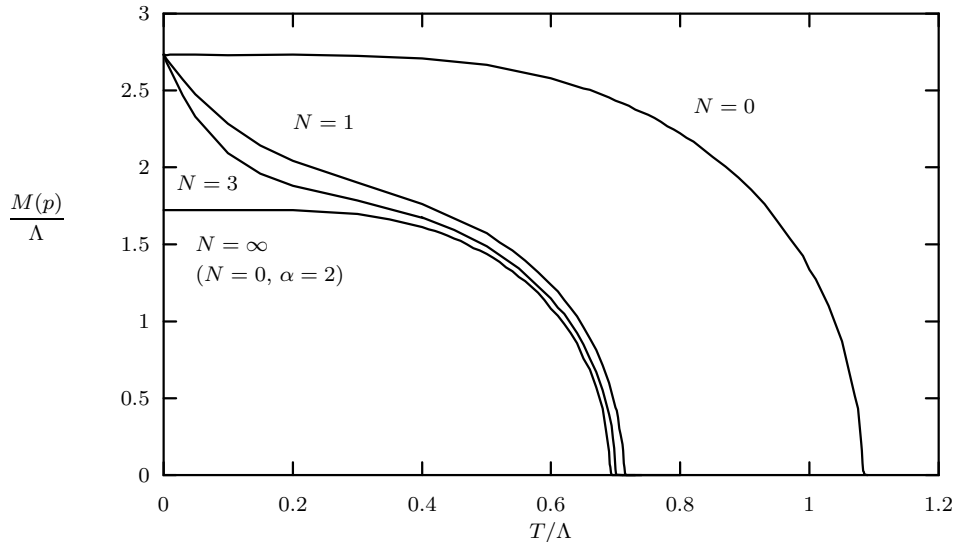


Figure 9: Dynamical fermion mass for $N = 0, N = 1, N = 3$ and $N = \infty$ as a function of the temperature T at $\alpha = 3$ and $p = 0.1\Lambda$.

7 Conclusion

We have investigated the mechanism of the chiral symmetry breaking in the strong-coupling Abelian gauge theories at finite temperature. The Schwinger-Dyson equation in Landau gauge is solved numerically within the framework of the instantaneous exchange approximation which is valid at high temperature. The effect of the hard thermal loop for the photon propagator on the phase transition has been also clarified. Here are our results in order:

1. The chiral phase transition is found to be of the 2nd order in the high temperature region. Thus the physical mass obeys the scaling law of the mean-field type. The effect of temperature on the chiral phase transition seems to be equivalent to the fermion loop effect in strong coupling QED at $T = 0$.
2. The critical temperature grows linearly as the critical coupling constant grows in the high temperature region. This result is opposed to that of Ref. [7] where they claimed that the chiral symmetry is always restored at finite temperature no matter how large the coupling constant is taken. The origin of this discrepancy lies in the vacuum polarization function. We have taken its transverse and longitudinal parts separately (see Eq. (28)) while in Ref. [7] they were assumed to be the same. Note that our choice of the function gives no constraints on the number of fermion flavors, whereas in strong coupling QED at $T = 0$ there might be the critical value N_c above which there is the chiral symmetric phase only [19].
3. The thermal photon mass reduces the effect of electromagnetic interaction. In the limit of the infinite number of fermion flavors the behavior of the mass function in the case with the thermal photon mass ($N = \infty$) is the same as in the case without the thermal photon mass ($N = 0$) with the coupling constant α replaced by $2\alpha/3$.

The next step that we should put forward is to extend our analysis to the one in the low temperature region. Along this line there are some difficulties to be overcome:

1. The vacuum polarization function at low temperature has to be estimated with some suitable approximation or in numerical calculations.

2. Proper approximations have to be found out in order to solve the Schwinger-Dyson equation at low temperature otherwise the equation is much complicated.

We expect that the structure of the chiral phase transition is the same as in the case we have investigated. This will be a subject in the forthcoming paper.

Acknowledgements

The authors would like to thank S. D. Odintsov for useful conversations in the early stage of the present work and K.-I. Kondo for enlightening discussions. The present work is performed under the auspice of Monbusho Fund (Grant-in-Aid for Scientific Research (C) and Grant-in-Aid for Encouragement of Young Scientists from the Ministry of Education, Science and Culture) with contract numbers 08640377(T.M.), 11640280(T.M.) and 11740154(T.I.) respectively.

Appendix

Here we argue the critical value of coupling constant α_c at vanishing temperature within the instantaneous exchange approximation, though this approximation is valid only at high temperature.

We begin with the linearized Schwinger-Dyson equation

$$M(p) = \frac{3\alpha}{4\pi p} \int_0^\Lambda dq M(q) \ln \frac{(p+q)^2}{(p-q)^2}, \quad (\text{A.1})$$

which is taken from Eq.(30) by setting $T = 0$ and neglecting the mass function in the denominator. If we take only the first term in the expansion of the logarithm,

$$\ln \frac{(p+q)^2}{(p-q)^2} = \sum_{n=0}^{\infty} \frac{4}{2n+1} \left[\left(\frac{q}{p}\right)^{2n+1} \theta(p-q) + \left(\frac{p}{q}\right)^{2n+1} \theta(q-p) \right], \quad (\text{A.2})$$

it is easily found that the Schwinger-Dyson equation,

$$M(p) \simeq \frac{3\alpha}{\pi p} \int_0^\Lambda dq M(q) \left[\frac{q}{p} \theta(p-q) + \frac{p}{q} \theta(q-p) \right], \quad (\text{A.3})$$

has the following nontrivial solution:

$$M(p) \propto p^\lambda, \quad (\text{A.4})$$

$$\lambda = \begin{cases} -1 + \sqrt{1 - \frac{6\alpha}{\pi}} & \left(0 < \alpha < \frac{\pi}{6}\right), \\ -1 \pm i\sqrt{\frac{6\alpha}{\pi} - 1} & \left(\alpha > \frac{\pi}{6}\right). \end{cases} \quad (\text{A.5})$$

Note that, when the value of coupling constant α lies in the region $\alpha < \pi/6$, λ is real and the system is in the symmetric phase, while the value of α lies in the region $\alpha > \pi/6$, λ is complex so that the solution of the Schwinger-Dyson equation is of the oscillatory function and the system is in the broken phase [3]. The critical value α_c in this case is $\pi/6$, which is half of the well known value $\pi/3$ in Landau gauge, because of the instantaneous exchange approximation and the simplification of the logarithm.

The evaluation of the critical value in the case including the full term of Eq.(A.2) is made as follows. The Schwinger-Dyson equation (A.1) with the expansion Eq.(A.2) reads

$$M(p) = \frac{3\alpha}{\pi p} \sum_{n=0}^{\infty} \frac{1}{2n+1} \int_0^\Lambda dq M(q) \left[\left(\frac{q}{p}\right)^{2n+1} \theta(p-q) + \left(\frac{p}{q}\right)^{2n+1} \theta(q-p) \right], \quad (\text{A.6})$$

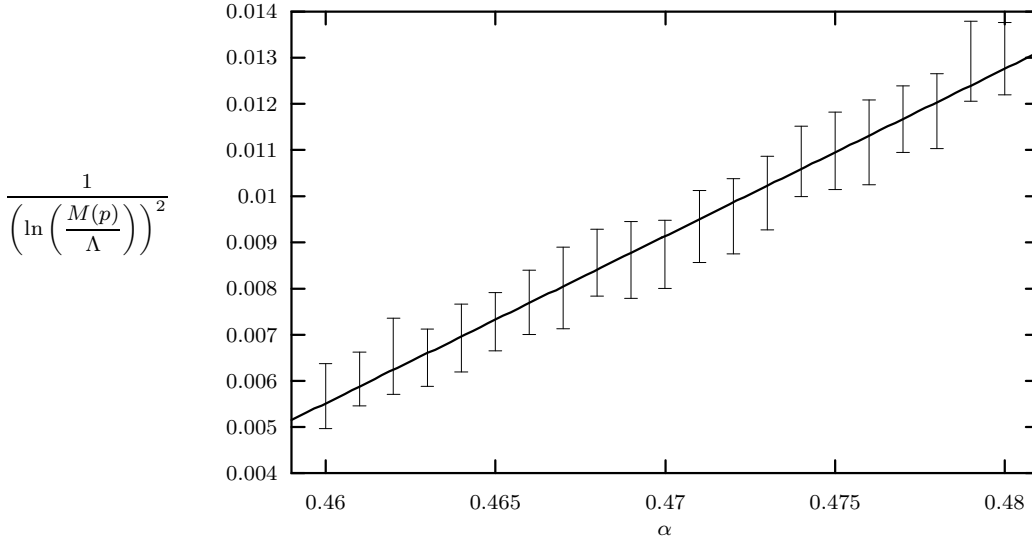


Figure 10: $1/(\ln(M(p)/\Lambda))^2$ vs. α with a fitted line. The critical value is given by $\alpha_c = 0.44477 \pm 0.00053$.

and we take the solution of the form $M(p) \propto p^\lambda$, which is valid in the above simplified case. Note that the value of λ is restricted by $-2 < \text{Re}\lambda < 0$ due to the condition that the integral in Eq.(A.6) should be finite. Then the Schwinger-Dyson equation reduces to

$$\frac{3\alpha}{2(\lambda+1)} \tan \frac{\pi(\lambda+1)}{2} = 1, \quad (\text{A.7})$$

by performing the integral and using the formula

$$\sum_{n=0}^{\infty} \frac{1}{(2n+1)^2 - x^2} = \frac{\pi}{4x} \tan \frac{\pi x}{2}. \quad (\text{A.8})$$

The real solution of Eq.(A.7) is easily found by considering the inclinations of $\tan \pi(\lambda+1)/2$ and $2(\lambda+1)/3$ at $\lambda = -1$. The result is that the nontrivial solution λ is real when $0 < \alpha < 4/(3\pi)$ which corresponds to the symmetric phase, whereas Eq.(A.7) has complex solutions when $\alpha > 4/(3\pi)$ which corresponds to the broken phase. Hence the critical value of coupling constant in this case is

$$\alpha_c = \frac{4}{3\pi} \quad (\text{A.9})$$

The exact value of critical coupling constant can be evaluated through numerical calculation, by fitting data with the function in the form of Miransky scaling law, and we find that the result is $\alpha_c \approx 0.445$. The numerical value 0.445 is in discrepancy with our theoretical prediction $4/(3\pi)$. It is easy to understand that this discrepancy is due to the fact that we made a linearization approximation. One should remember that the mass function in the denominator in Eq.(30) is neglected in Eq.(A.1). This means that the exact value of α_c must be slightly larger than $4/(3\pi)$ and would be in the range

$$\frac{4}{3\pi} < \alpha_c \lesssim \frac{\pi}{6}. \quad (\text{A.10})$$

It is easy to see that our numerical result satisfies this speculation.

References

- [1] M. Baker, K. Johnson and R. S. Willey, *Phys. Rev. Lett.* **11** (1963) 518; *Phys. Rev.* **136** (1964) B1111; **163**(1967) 1699.
- [2] T. Maskawa and H. Nakajima, *Prog. Theor. Phys.* **52** (1974) 1326; **54** (1975) 860.
- [3] R. Fukuda and T. Kugo, *Nucl. Phys.* **B117** (1976) 250.
- [4] See, e. g. V. A. Miransky, *Dynamical Symmetry Breaking in Quantum Field Theories*, World Scientific Pub. Co. (1993) for a full list of references.
- [5] F. J. Dyson, *Phys. Rev.* **75** (1949) 1736;
J.Schwinger, *Proc. Nat. Acad. Sc.* **37** (1951) 452,455.
- [6] T. Akiba, *Phys. Rev.* **D36** (1987) 1905.
- [7] K.-I. Kondo and H. Yoshida, *Int. J. Mod. Phys.* **A10** (1995) 199.
- [8] G. Triantaphyllou, *Phys. Rev.* **D58** (1998) 065006.
- [9] H. Umezawa, H. Matsumoto and M. Tachiki, *Thermo Field Dynamics and Condensed States*, North-Holland Pub. Co. (1982).
- [10] J. I. Kapusta, *Finite Temperature Field Theory*, Cambridge University Press (1989).
- [11] M. Le Bellac, *Thermal Field Theory*, Cambridge University Press (1996).
- [12] A. Das, *Finite Temperature Field Theory*, World Scientific Pub. Co. (1997).
- [13] S. Weinberg, *Phys. Rev.* **D9** (1974) 335;
L. Dolan and R. Jackiw, *Phys. Rev.* **D9** (1974) 3320.
- [14] K. B. Joseph, *Phys. Lett.* **B115** (1982) 252;
D. Bailin, J. Cleymans and M. D. Scadron, *Phys. Rev.* **D31** (1985) 164;
S. K. Kang, W.-H. Kye and J. K. Kim, *Phys. Lett.* **B299** (1993) 358.
- [15] Y. Taniguchi and Y. Yoshida, *Phys. Rev.* **D55** (1997) 2283.
- [16] D. J. Gross and A. Neveu, *Phys. Rev.* **D10** (1974) 3235.
- [17] H. O. Wada, *Lett. Nuovo Cimento* **11** (1974) 697;
L. Jacobs, *Phys. Rev.* **D10** (1974) 3956;
R. F. Dashen, S. Ma and R. Rajaraman, *Phys. Rev.* **D11** (1975) 1499;
D. J. Harrington and A. Yildiz, *Phys. Rev.* **D11** (1975) 779;
W. Dittrich and B.-G. Englert, *Nucl. Phys.* **B179** (1981) 85.
- [18] T. Inagaki, T. Koumo and T. Muta, *Int. J. Mod. Phys.* **A10** (1995) 2241.
- [19] K.-I. Kondo and H. Nakatani, *Nucl. Phys.* **B351** (1991) 236; *Prog. Theor. Phys.* **88** (1992) 737.